T-EMC/36/1//14318D

A Comparison of Telemetry Signals in the Presence and Absence of a Subcarrier

Mazen M. Shihabi
Tien Manh Nguyen
Sami M. Hinedi

Reprinted from
IEEE TRANSACTIONS ON ELECTROMAGNETIC COMPATIBILITY
Vol. 36, No. 1, February 1994

A Comparison of Telemetry Signals in the Presence and Absence of a Subcarrier

Mazen M. Shihabi, *Student Member, IEEE*, Tien Manh Nguyen, *Senior Member, IEEE*, and Sami M. Hinedi, *Member, IEEE*

Abstract— **The performance of deep-space telemetry signals that employ a residual carrier modulation technique is compared in the presence and absence of a subcarrier. When the subcarrier is present, the performance for the resulting pulse-coded modulation/phase-shift keyed/phase-modulated (PCM/PSK/PM) scheme is evaluated for both sine-wave and square-wave subcarriers and non-return-to zero (NRZ) data. When the subcarrier is absent, the performance for the resulting PCM/PM technique is evaluated for both the NRZ and the bi-phase data format. The comparison is based on telemetry performance as well as bandwidth efficiency. The first criterion is characterized in terms of the symbol error rate (SER) as a function of symbol SNR, loop bandwidth-to-data rate ratio, and modulation index. The bandwidth efficiency is characterized by the occupancy factor. The results of both the analysis and measurements show that when the interference-to-carrier ratio (ICR) is less than −20 dB, the performance degradation in the absence of a subcarrier is negligible. Various combinations of loop bandwidth-to-data rate ratios and modulation indices that achieve this performance are derived and listed. Bandwidth occupancy comparison indicates that PCM/PM/NRZ is the most efficient in this regard. Therefore, by eliminating the subcarrier and using the PCM/PM/NRZ scheme, many advantages can be realized without any sacrifice in performance.**

I. Introduction

In the past, when space missions operated at low data rates using residual carrier modulation, it was necessary to separate the data from the residual carrier to avoid interference. This was achieved by placing the data modulation on a subcarrier since direct modulation of the data on the carrier would cause most of the data power to fall within the bandwidth of the carrier phase-lock loop (PLL) and, as a consequence, interfere with its operation. The scheme in which the data are phase-shift keyed (PSK) onto a subcarrier and then phase-modulated (PM) onto a sinusoidal carrier is called the PCM/PSK/PM modulation scheme. However, space missions and the Deep Space Network (DSN) supporting them have evolved over the years and will soon be capable of supporting very high data rates, on the order of tens of megabits per second [1, ch. 3]. At these higher data rates, the data signal spectrum is broad, and therefore, if the subcarrier were to be eliminated, the part of the spectrum that would fall within the carrier loop bandwidth would be flat and appear as white noise to a narrow loop. Since the ratio of loop bandwidth to data rate is very small at high data rates, it would seem that this additional white noise component would degrade the tracking performance very little. This latter scheme in which the telemetry data are phase-modulated directly onto the carrier is known as the PCM/PM modulation scheme.

In this paper, it is shown that the use of the PCM/PM technique under appropriate conditions will reap many advantages without sacrificing performance. Foremost among these advantages is the lower bandwidth, which can be extremely useful when antenna arraying is employed or when tracking multiple spacecraft signals within the field of view of a single antenna. In the latter case, the various signals can be separated in the frequency domain and a single receiver front end can be used to downconvert them to baseband. This idea is very similar to frequency division multiplexing (FDM) except that the carriers are generated by different oscillators. Secondly, PCM/PM has the advantage of eliminating subcarrier loss in the receiver. Finally, the presence of the residual carrier provides useful data for navigation purposes and also safeguards the investment made in PLL receivers by the DSN and other space agencies. In light of the above factors, the goal of this paper is to assess and compare the performance degradation in DSN receivers due to the interference between the data and the residual carrier for the above two schemes. For the PCM/PM modulation scheme, two kinds of data formats are considered. The non-return-to-zero (NRZ) format and the Manchester (or bi-phase) data format. For the PCM/PSK/PM modulation scheme, the performance is determined for the two most commonly used subcarriers: the sine-wave, which is used for near-Earth missions (category A) and the square-wave, which is used for deep-space missions (category B), as recommended by the Consultative Committee for Space Data Systems (CCSDS) [2]. The comparison is based on the telemetry symbol error rate (SER) and the bandwidth occupancy (BW). Throughout this paper, it is assumed that the data are not encoded. Hence, the SER is equivalent to the bit error rate (BER), and the two terms are used interchangeably.

The paper is organized as follows: A brief description of the various residual carrier modulation schemes is presented in Section II. The general analysis and summary of the theoretical results are presented in Section III. The discussion and comparison of theoretical and measured performance are

Manuscript received April 12, 1993; revised August 4, 1993. The research described in this paper was carried out by Jet Propulsion Laboratory, California Institute of Technology, under Contract with the National Aeronautics and Space Administration.

The authors are with Jet Propulsion Laboratory, California Institute of Technology, Pasadena, CA 91109.

IEEE Log Number 9214318.

carried out in Section IV, followed by the conclusion in Section V.

II. Description of the Residual Carrier Modulation Techniques

The telemetry signal in the two schemes can be represented mathematically by

$$s(t) = \sqrt{2P_T}\sin[\omega_c t + mP(t)d(t)] \tag{1}$$

where P_T is the total power; ω_c is the angular carrier frequency in radians per second; m is the modulation index in radians $(0 < m < \pi/2)$; $d(t)$ is the binary data sequence with symbol rate $R_s = 1/T_s$; and

$$P(t) = \begin{cases} 1, & \text{PCM/PM} \\ \text{sqr}\,(\omega_{sc}t + \theta_{sc}), & \text{PCM/PSK/PM} \\ & \text{(square-wave)} \\ \sin\,(\omega_{sc}t + \theta_{sc}), & \text{PCM/PSK/PM} \\ & \text{(sine-wave).} \end{cases}$$

A. The PCM/PM Technique

There is no subcarrier used in this scheme, hence one substitutes 1 for $P(t)$ in (1), obtaining

$$s(t) = \sqrt{2P_T}\,\sin\,[\omega_c t + md(t)]. \tag{2}$$

The received signal, $r(t)$, is corrupted by additive white Gaussian noise (AWGN), $n(t)$, with one-sided power spectral density N_0 (W/Hz). By using simple trigonometric identities, the received signal can be expanded as

$$\begin{aligned} r(t) = \sqrt{2P_T}\,&[\cos\,(m)\sin\,(\omega_c t + \theta_c) \\ &+ d(t)\sin\,(m)\cos(\omega_c t + \theta_c)] + n(t) \end{aligned} \tag{3}$$

where θ_c is the carrier phase. The first and second terms of (3) are the residual carrier components $C(t)$ and the data components $I_c(t)$, respectively. Explicitly,

$$C(t) = \sqrt{2P_T}\cos\,(m)\sin\,(\omega_c t + \theta_c) \tag{4a}$$

$$I_c(t) = \sqrt{2P_T}d(t)\sin\,(m)\cos\,(\omega_c t + \theta_c). \tag{4b}$$

The data component is denoted by $I_c(t)$ to explicitly indicate its role as the interfering component to the carrier PLL. It is seen that the modulation index m has allocated the total transmitted power to the carrier and to the data channel, where the carrier power and data power are respectively given by

$$P_C = P_T\cos^2 m \tag{5a}$$

$$P_D = P_T\sin^2 m \tag{5b}$$

Another important parameter is the power spectral density (PSD) of the transmitted signal. From (2), it is easy to determine that the one-sided PSD of the transmitted signal in the PCM/PM scheme is equal to

$$S(f) = P_T\,[\cos^2\,(m)\delta(f - f_c) + \sin^2\,(m)S_D(f - f_c)] \tag{6}$$

where $S_D(f)$ is the PSD of the data sequence and is given by Yuen [1] and Holmes [3]

$$S_D(f) = \begin{cases} 1/R_s\ \dfrac{\sin^2\,(\pi f/R_s)}{(\pi f/R_s)^2}, & \text{NRZ data} \\ 1/R_s\ \dfrac{\sin^2\,(\pi f/2R_s)}{(\pi f/2R_s)^2}, & \text{bi-phase data} \end{cases} \tag{7}$$

By substituting in (6), one obtains expressions for the spectrum of the transmitted signal for these two cases, as shown in Fig. 1(a) and (b), respectively. Because of the symmetrical nature of the spectrum around the origin, only the positive frequency portions are shown in the plots.

B. The PCM/PSK/PM Technique

This scheme is the traditional residual carrier technique, where a subcarrier is used to separate the data from the carrier. The telemetry signal is given in (1) and results in

$$\begin{aligned} s(t) = \sqrt{2P_T}\,&[\cos\,(mP(t))\sin\,(\omega_c t) \\ &+ d(t)\sin\,(mP(t))\cos(\omega_c t)] \end{aligned} \tag{8a}$$

where $d(t)$ is the NRZ binary data sequence, and $P(t)$ is the subcarrier waveform. Using (8a), an expression for the PSD of the transmitted signal is derived in [4] for the two subcarrier waveforms used in space applications. When $P(t)$ is a unit-power square-wave subcarrier of frequency f_{sc}, (8a) reduces to

$$\begin{aligned} s(t) = \sqrt{2P_T}\,&[\cos\,(m)\sin\,(\omega_c t) \\ &+ d(t)P(t)\sin\,(m)\cos\,(\omega_c t)]. \end{aligned} \tag{8b}$$

The power spectral density for this case is given by

$$\begin{aligned} S(f) = P_T\{&\cos^2\,(m)\delta(f - f_c) \\ &+ \left(\frac{4}{\pi^2}\right)\sin^2(m)\sum_{k\geq 1}\Big[[S_D(f - f_c - (2k-1)f_{sc}) \\ &+ S_D(f - f_c + (2k-1)f_{sc})]/(2k-1)^2\Big]\Big\} \end{aligned} \tag{9}$$

where $S_D(f)$ is the PSD of the NRZ binary data sequence which was defined earlier in (7). The first term in (9) is the residual carrier spectral component, and the second term is the data component. The plot of (9) is shown in Fig. 1(c). The CCSDS recommends that the subcarrier frequency-to-bit rate, $n = f_{sc}/R_s$, be an integer [2] where R_s is the data rate. On the other hand, when $P(t)$ is a sine-wave subcarrier, the power spectral density of the telemetry signal is given by

$$\begin{aligned} S(f) = P_T[&J_0^2(m)\delta(f - f_c) \\ &+ \sum_{i\ \text{even}} J_i^2(m)[\delta(f - f_c - if_{sc}) + \delta(f - f_c + if_{sc})] \\ &+ \sum_{k\ \text{odd}} J_k^2(m)[S_D(f - f_c - kf_{sc}) \\ &+ S_D(f - f_c + kf_{sc})]] \end{aligned} \tag{10}$$

where $J_k(\cdot)$ is the kth-order Bessel function. The first term in (10) is the residual carrier spectral component, the second term is the intermodulation loss component, and the third term is the data component.

III. Performance Analysis

On the ground, the carrier component $C(t)$ of the received signal $s(t)$ is tracked by the PLL. The tracking performance of the PLL depends on the modulation index m and the tracking loop noise bandwidth-to-data rate ratio (B_L/R_S). Fig. 1(a)

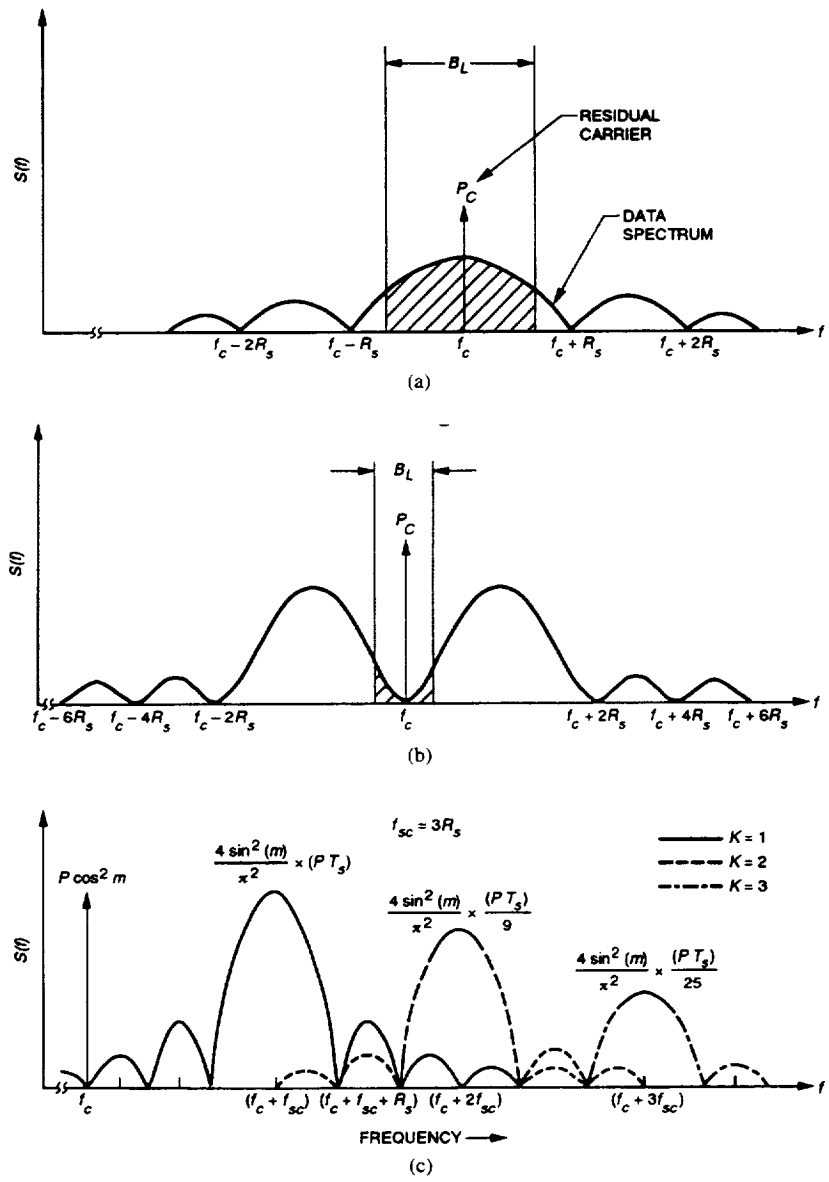

Fig. 1. Interaction between the residual carrier and the data spectrum. (a) Interaction between the residual carrier and the NRZ data spectrum when $B_L < R_S$. (b) Interaction between the residual carrier and the bi-phase data spectrum when $B_L < R_S$. (c) Power spectrum of the residual carrier with square-wave as its subcarrier.

and (b) illustrates the spectrum of the PCM/PM signals and the portion (shaded area) of the data spectrum that lies within the carrier loop bandwidth B_L. From these diagrams, it is clear that the interference power is a function of both B_L and R_S. The performance of the carrier-tracking loop in the presence of the data is characterized by the interference-to-carrier signal power ratio (ICR). This ratio is determined for all schemes, and the effect of this interference on the phase error process is assessed. Consequently, the SER is calculated for all cases. In order to proceed, a few parameters must be identified. First, the one-sided loop bandwidth of the PLL is defined in terms of the carrier-tracking loop transfer function $H(j2\pi f)$, as follows:

$$B_L = \int_0^\infty |H(j2\pi f)|^2 \, df. \tag{11}$$

Current DSN receivers typically use passive second-order PLL filters resulting in [4]

$$|H(f)|^2 = \frac{1 + 2(f/f_n)^2}{1 + (f/f_n)^4} \tag{12}$$

where f_n is the loop natural frequency and is related to the one-sided loop noise bandwidth B_L through

$$B_L = \pi f_n \left(\xi + \frac{1}{4\xi}\right) \tag{13}$$

with ξ denoting the damping factor (typically $\xi = 0.707$ is used). Next, the ICR is determined for the various schemes.

A. Determination of the ICR

From (1) and Fig. 1, the interference power is that portion of the data spectrum that falls within the carrier loop bandwidth

and interferes with the carrier power, as given by (5). Thus the ICR becomes

$$\text{ICR} = \tan^2(m) \int_0^\infty |H(j2\pi f)|^2 S_D(f)\, df. \quad (14)$$

Depending on the data format and rate, (14) can be simplified further.

1) PCM/PM with Ideal NRZ Data Format: By substituting (7), (12), and (13) into (14) and evaluating the integral, one obtains

$$\text{ICR} = \tan^2(m)\left[\frac{1}{2} + \frac{1}{4\gamma\sqrt{2}}(1 - e^{-\gamma\sqrt{2}} \cdot (\cos(\gamma\sqrt{2}) + 3\sin(\gamma\sqrt{2})))\right] \quad (15)$$

where

$$\gamma \triangleq \frac{B_L}{R_S}. \quad (16)$$

The upper and lower bounds for the ICR can be found from (15). If one lets γ approach zero (i.e., the data rate R_S approaches infinity) and by using L'Hospital's rule, one gets the lower bound

$$\text{ICR} = 0. \quad (17)$$

On the other hand, if one lets γ approach infinity (R_S approaches zero), then one obtains the upper bound

$$\text{ICR} = \frac{\tan^2(m)}{2}. \quad (18)$$

From these bounds, it is clear that as the loop bandwidth-to-data rate ratio, γ, increases, the ICR increases. These results are obvious from Fig. 1(a) and (b), because as B_L increases, the shaded area representing the interference due to the data increases while the residual carrier power P_c remains unchanged. Also from (15), one notices that for a fixed γ, the ICR increases as m increases, since for a fixed total power P_T, P_c decreases as m increases (remember $0 < m < \pi/2$) while P_D increases. Using (15), the ICR is plotted in Fig. 2(a) as a function of γ for different values of m. The appropriate values of γ can be determined for a given modulation index m so that the ICR does not exceed the maximum allowable value. For a deep-space mission, the maximum allowable interference for the carrier tracking is $(\text{ICR})_{\max} = -15$ dB, as recommended by the International Radio Consultative Committee (CCIR) [5]. Note that this value was derived based on the CW interference scenario. Another important parameter is the critical value of γ (for a given m) that will cause the ICR to reach its maximum allowable value. These critical values for γ as a function of m are plotted in Fig. 2(b). The region on this graph corresponding to values of γ that yield an ICR ratio below the maximum allowable value is called the operating region (OR). From Fig. 2(b), one can see that γ decreases as m increases in order to keep the ICR fixed.

For the NRZ data format case, determining the performance is of interest in the following two special cases. For the high data rate case, the data power spectrum that falls into the carrier tracking loop bandwidth is essentially constant over the tracking loop bandwidth. Thus for $\gamma < 0.1$, the interference

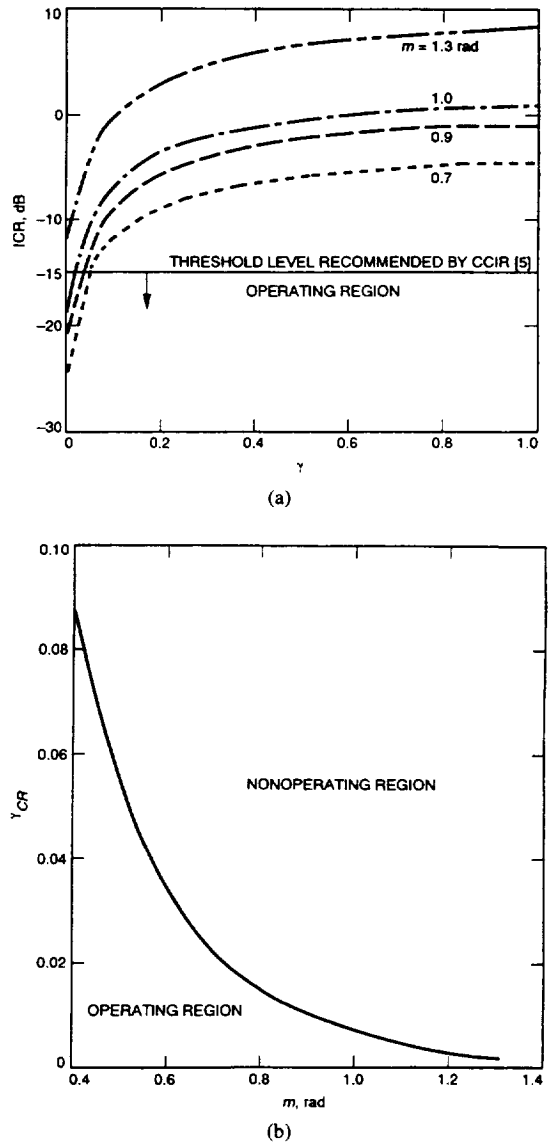

Fig. 2. Effects of interference due to the NRZ data format. (a) ICR versus γ for the PCM/PM/NRZ scheme. (b) γ versus modulation index m when ICR = -15 dB for the PCM/PM/NRZ case.

can be considered as additional additive white noise and (14) can be approximated by

$$\text{ICR} \approx \tan^2(m) S_D(0) \int_0^\infty |H(f)|^2\, df \quad (19)$$

or

$$\text{ICR} \approx \left(\frac{B_L}{R_S}\right)\tan^2(m) \quad \text{when } \frac{B_L}{R_S} < 0.1. \quad (20)$$

For the low data rate case, all the power of the interference component falls within the carrier tracking loop bandwidth. Thus the ICR can be approximated by

$$\text{ICR} \approx \tan^2(m)\frac{1}{R_S}\int_0^{B_L} \frac{\sin^2(\pi f/R_S)}{(\pi f/R_S)^2}\, df. \quad (21)$$

When $B_L/R_S > 10$, the above integral is easily evaluated:

$$\text{ICR} \approx \left(\frac{1}{2}\right)\tan^2(m). \quad (22)$$

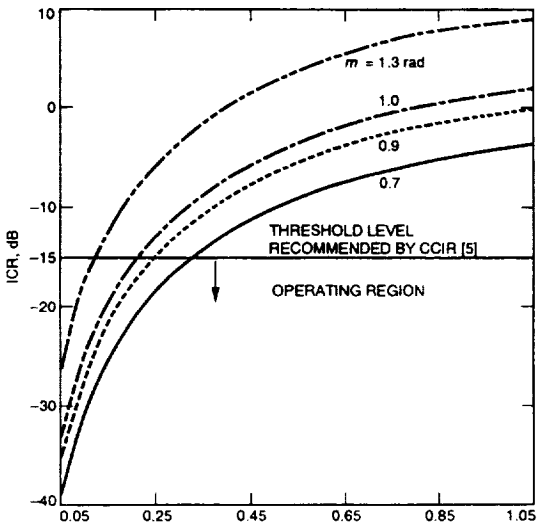

(a)

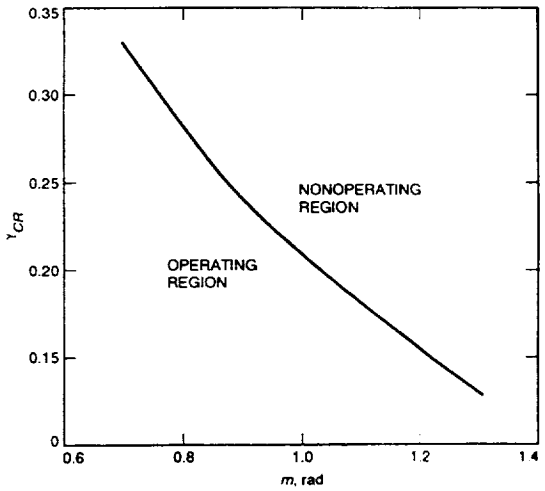

(b)

Fig. 3. Effects of interference due to bi-phase data format. (a) ICR versus γ for the PCM/PM/bi-phase scheme. (b) γ versus modulation index m when ICR = −15 dB for the PCM/PM/bi-phase case.

In practice, the above case is possible when a data rate of 32 symbols/s is transmitted and a wide carrier tracking mode at $2B_L = 300$ Hz is selected by the ground station receiver.

2) PCM/PM With Bi-Phase Data Format: By substituting (7) for the bi-phase spectrum and (12) into (14) and evaluating the integral, one obtains

$$\begin{aligned}\text{ICR} &= \tan^2(m)\left[\frac{1}{2}+\frac{9}{16\gamma}\right.\\ &\quad -\frac{3}{4\gamma}e^{-2\gamma/3}\left(\cos\left(\frac{2\gamma}{3}\right)+3\sin\left(\frac{2\gamma}{3}\right)\right)\\ &\quad \left.+\frac{3}{16\gamma}e^{-4\gamma/3}\left(\cos\left(\frac{4\gamma}{3}\right)+3\sin\left(\frac{4\gamma}{3}\right)\right)\right]. \quad (23)\end{aligned}$$

The above ICR is plotted in Fig. 3(a) as a function of γ for various values of m. The corresponding operating region for the ratio γ is plotted in Fig. 3(b).

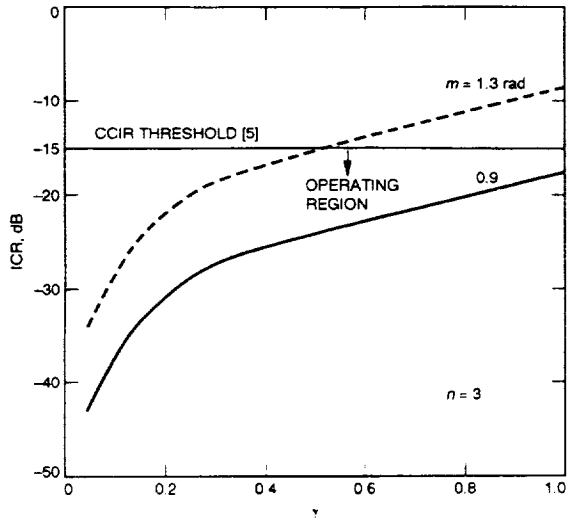

Fig. 4. ICR versus γ for the PCM/PSK/PM scheme with square-wave subcarrier

3) PCM/PSK/PM: This scheme is used to separate the residual carrier and the data components so that the interference caused by the data to the residual carrier is minimized. The higher the subcarrier-frequency-to-data rate ratio the lower the interference. The ICR will be derived for the case of the square-wave subcarrier, and the results can be extended to the sine-wave case very easily. The data component spectrum can be extracted from the transmitted signal spectrum, as given by (9), and is equal to

$$\begin{aligned}S_{\text{Data}}(f) = \left(\frac{4}{\pi^2}\right)\sum_{k\geq 1}&[S_D(f-f_c-(2k-1)f_{sc})\\ &+S_D(f-f_c+(2k-1)f_{sc})]/(2k-1)^2] \quad (24)\end{aligned}$$

where $S_D(f)$ is given in (7), and $f_{sc} = n \times R_s$. By substituting (13) and (24) in (14) and evaluating the integral numerically for the case when $n = 3$, one obtains values for the ICR as a function of γ when the modulation index m is chosen to have the values 0.9 and 1.3 rad, respectively. The results are plotted in Fig. 4 where it is found that when $m = 0.9$ rad and $\gamma \leq 1$, the ICR never reaches the maximum allowable value. However, a critical value of $(\gamma)_{CR} = 0.56$ is found when the modulation index is increased to $m = 1.3$ rad. In Fig. 4, it is shown that the ICR decreases rapidly for the two modulation indices when $\gamma \leq 0.2$. The above procedure was repeated for $n \geq 3$ and it was found that the interference is negligible. Note that for the PCM/PSK/PM scheme, the critical value for γ is quite large, even at the largest modulation index chosen, $m = 1.3$ rad. The same cannot be said about the PCM/PM scheme where one must operate at values of γ much below 1, in order to keep the ICR below −15 dB.

B. The Effect of the Interference on Carrier-Tracking Phase Error

When the received signal is tracked by a PLL, the phase error process, defined as

$$\phi(t) = \theta(t) - \hat{\theta}(t) \quad (25)$$

has contributions from both the thermal noise and the interference caused by the data. The accuracy of the estimate $\hat{\theta}(t)$ is dependent on the power allocated to the residual carrier component. Under the high-data-rate assumption, the data interference component has a spectrum over the PLL bandwidth, and hence it can be considered as an additional additive white noise. In this case, the variance of the phase error due to the combined additive Gaussian noise is given by [6]

$$\sigma^2 = \frac{NB_L}{P_c} \tag{26}$$

where N is the effective noise spectral density resulting from thermal noise and data interference, and is determined as follows:

$$N = \frac{1}{B_L}\int_0^\infty |H(j2\pi f)|^2[N_0 + P_D S_D(f)]df \tag{27}$$

Alternatively, one has

$$N = N_0 + \frac{P_D}{B_L}\alpha \tag{28}$$

where

$$\alpha \triangleq \int_0^\infty S_D(f)|H(j2\pi f)|^2\, df. \tag{29}$$

Rather than expressing the variance of the phase error in terms of the modified noise spectral density N it is expressed in terms of the ICR to show the interdependence explicitly. Thus under the high-data-rate assumption, the variance of the carrier-tracking phase error becomes [7]

$$\sigma^2 = \frac{1}{\rho} = \frac{1}{\rho_0} + \text{ ICR} \tag{30}$$

where ρ is the effective loop SNR, and ρ_0 is the carrier loop signal-to-thermal-noise power ratio defined as

$$\rho_0 = \frac{P_C}{N_0 B_L} = \frac{E_S/N_0}{(B_L/R_S)\times \tan^2(m)}. \tag{31}$$

Under the linear operation assumption, the probability density function (pdf) of the phase error process may be approximated by the Tikhonov pdf [1]. Hence the pdf of $\phi(t)$ is completely determined, once ρ is known, from

$$p(\phi) = \frac{\exp(\rho\cos\phi)}{2\pi I_0(\rho)}, \quad \text{when } -\pi \le \phi \le \pi \tag{32}$$

where $I_0(\cdot)$ is the modified Bessel function of the first kind, and ρ is the effective loop SNR, which is the inverse of the variance σ^2 of the carrier tracking phase error. Now, this variance for all cases must be found.

1) PCM/PM with Ideal NRZ Data Format: For the NRZ data format, the performance will be determined for the low-data-rate case as well as the high-data-rate case.

a) High-Data-Rate Case (B_L / R_S < 0.1): The expression for the ICR for this case is found in (20), which when substituted in (30), gives the phase error variance

$$\sigma^2 = \frac{1}{\rho} \approx \frac{1}{\rho_0} + \left(\frac{B_L}{R_S}\right)\tan^2(m). \tag{33}$$

The inverse of the phase error variance, i.e., the effective loop SNR as a function of symbol SNR (SSNR) is plotted in Fig. 5(a) and (b) for this case. The region corresponding to values of $\rho < 8$ dB is called the PLL nonoperating region (PLLNOR). This is the region where the loop is slipping cycles and should be avoided.

b) Very Low-Data-Rate Case (B_L / R_S > 10: Here one cannot treat the data interference as just additional white noise, but rather the procedure chosen by Youn and Lindsey [8] will be followed. When the data rate is very low, the carrier interference component $I_C(t)$ can be treated as CW interference with its phase switching slowly and randomly between 0 and π with respect to the phase of the residual carrier. Thus if one lets $\Delta\theta$ be the phase difference between the interference component $I_C(t)$ and the carrier component $C(t)$, then within the tracking loop bandwidth, $\Delta\theta$ will take on the values 0 and π with equal probability. The Fokker–Plank method can be used to derive the pdf for the carrier-tracking phase error. Let ϕ denote the carrier-tracking phase error induced by $I_C(t)$ and the AWGN, $n(t)$. Then the conditional pdf $p(\phi|\Delta\theta)$ in the presence of CW interference can be approximated as

$$P_W(\phi|\Delta\theta) \cong \left[\frac{\exp[-(\phi - M)^2/2\sigma^2]}{\sqrt{2\pi\sigma^2}\,\text{erf}\left(\pi/\sqrt{2\sigma^2}\right)}\right], \quad \text{for } |\phi| \le \pi \tag{34}$$

where M and σ^2 are the conditional mean and variance of the phase error, ϕ, respectively, and they are defined as

$$M = -\frac{\sqrt{\text{ICR}}\sin(\Delta\theta)}{1 + \left(\sqrt{\text{ICR}}\cos(\Delta\theta)\right)} \tag{35}$$

and

$$\sigma^2 = \frac{1}{\rho_0[1 + \sqrt{\text{ICR}}\cos(\Delta\theta)]}. \tag{36}$$

By using Bayes' rule, the conditioning on $\Delta\theta$ can be removed to obtain the pdf of the phase error process

$$p(\phi) = \frac{1}{2}\left[\frac{\exp[-\phi^2/2\sigma_+^2]}{\sqrt{2\pi\sigma_+^2}\,\text{erf}(\pi/\sqrt{2\sigma_+^2})} + \frac{\exp[-\phi^2/2\sigma_-^2]}{\sqrt{2\pi\sigma_-^2}\,\text{erf}(\pi/\sqrt{2\sigma_-^2})}\right] \tag{37}$$

where

$$\sigma_\pm^2 = \frac{1}{\rho_0\left(1 \pm \sqrt{\text{ICR}}\right)}. \tag{38}$$

The above approximation is valid only when the ICR < 1, which is the case of interest here. The effective loop SNR is

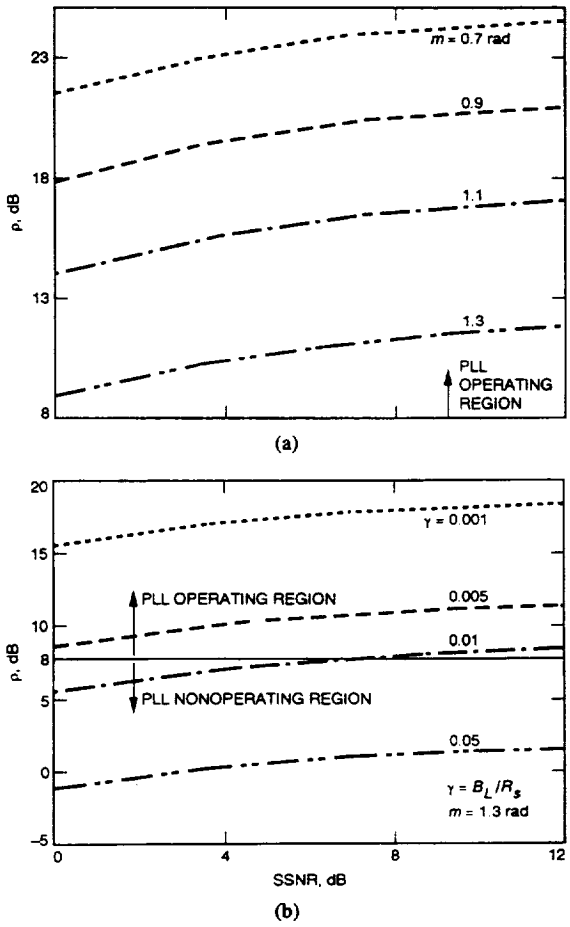

Fig. 5. Effective loop SNR as a function of SSNR and m for PCM/PM/NRZ. (a) Effective loop SNR versus SSNR for PCM/PM/NRZ ($\gamma = 0.005$). (b) Effective loop SNR versus symbol SNR fir PCM/PM/NRZ ($m = 1.3$ rad).

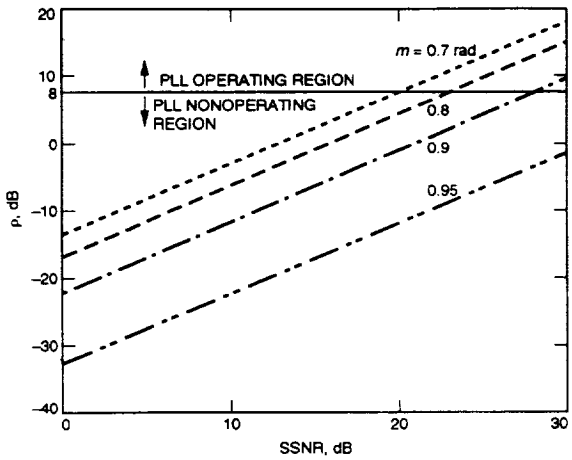

Fig. 6. Effective loop SNR versus SSNR for PCM/PM/NRZ ($\gamma = 10$), low-data-rate case.

depicted in Fig. 6 as a function of the SSNR when $\gamma = 10$. The above pdf will be used to derive the SER for the low-data-rate case instead of the Tikhonov pdf that is used in the high-data-rate case.

2) PCM/PM With Ideal Bi-phase Data Format: Under the high-data-rate assumption, the variance of the phase error

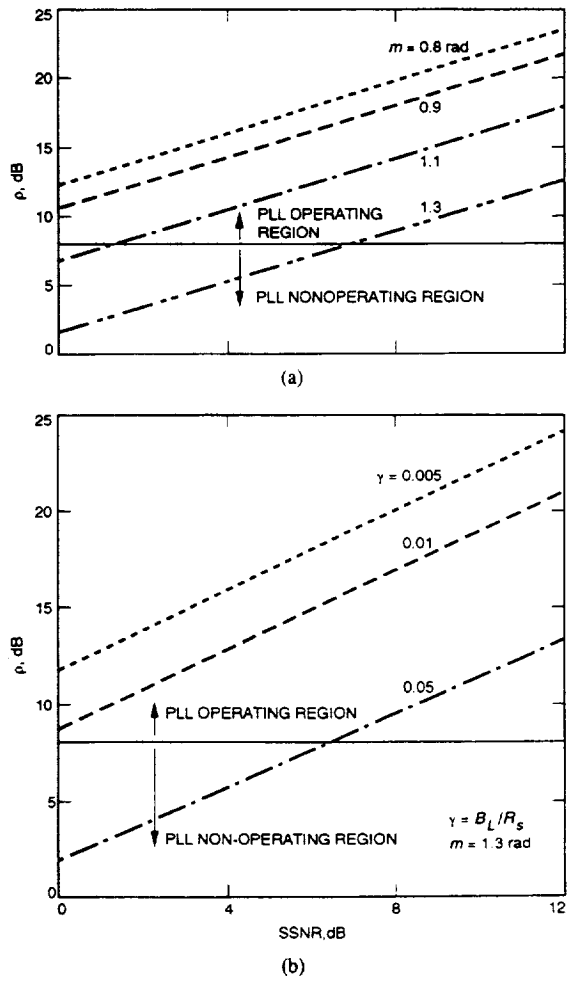

Fig. 7. Effective loop SNR as a function of SNR for PCM/PM/bi-phase ($\gamma = 0.05$). (b) Effective loop SNR versus SSNR for PCM/PM/bi-phase ($m = 1.3$ rad).

process is given earlier in (30). By substituting the expression for the ICR derived in (23), the variance is determined, and consequently the Tikhonov pdf is now completely characterized. As mentioned before, in order to specify the PLL operating region, the inverse of the phase error variance is plotted as a function of SSNR in Fig. 7(a) and (b) for different modulation indices.

3) PCM/PSK/PM: By substituting the numerical values for the ICR obtained in Section III-A.3) when $m = 1.3$ rad and the ratio $B_L/R_S = 0.05$ in (30), one obtains the phase error variance for the square-wave subcarrier. The rms of this variance is plotted as a function of loop SNR ρ_0 in Fig. 8 for $n = 1$ and $n = 3$, where n is the subcarrier frequency-to-bit rate, as defined earlier. The figure indicates that if one chooses the integer $n \geq 3$, the performance of this scheme is almost identical to that of the ideal case. The ideal case refers to the binary phase-shift-keying (BPSK) modulation scheme over an AWGN channel.

C. Effect of Interference on the SER Performance

The symbol error probability for uncoded PSK transmission over a Gaussian channel disturbed by additive white noise of

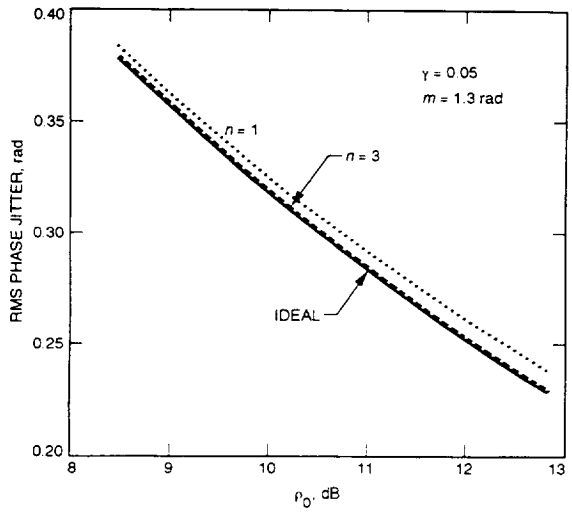

Fig. 8. RMS of phase jitter for the PCM/PM/PSK square-wave case.

one-sided spectral thermal noise density, N_0, is given by [1, ch. 5]

$$P_S = \frac{1}{2}\ \text{erfc}\left(\sqrt{\frac{E_S}{N_0}}\right). \tag{39}$$

The conditional symbol error probability that takes into account the phase error process is given by [6]

$$P_S(\phi) = \frac{1}{2}\ \text{erfc}\left(\sqrt{\frac{E_S}{N_0}}Y(\phi)\right) \tag{40}$$

where

$$Y(\phi) = \frac{1}{T_S}\int_0^{T_S} \cos\left[\phi(t)\right]\, dt. \tag{41}$$

Then the unconditional symbol error probability can be obtained by averaging $P_S(\phi)$ over ϕ, i.e.,

$$P_S = \int_{-\pi}^{\pi} P_S(\phi)\, p(\phi)\, d\phi. \tag{42}$$

1) PCM/PM with Ideal NRZ Data Format:

a) High-data-rate case: When the data rate is high with respect to the receiver tracking loop bandwidth (i.e., $\gamma < 0.1$), the phase error process $\phi(t)$ varies slowly and is essentially constant over a symbol interval, T_S. Then from (41), it is concluded that for this case

$$Y(\phi) \approx \cos\ \phi \tag{43}$$

and the average symbol error probability is obtained by substituting (43) in (42) to give

$$P_S = \frac{1}{2}\int_{-\pi}^{\pi} \text{erfc}\left(\sqrt{\frac{E_S}{N_0}}\cos\phi\right)\frac{\exp\left(\rho\cos\phi\right)}{2\pi I_0(\rho)}\, d\phi. \tag{44}$$

This SER, P_S, is plotted in Fig. 9(a) as a function of SSNR (E_S/N_0) for different values of m when $\gamma = 0.005$. From this figure, one sees that when $m = 1.3$ rad, the degradation becomes considerable. Fig. 9(b) depicts that even when $m = 1.3$ rad, the performance can be improved by decreasing γ,

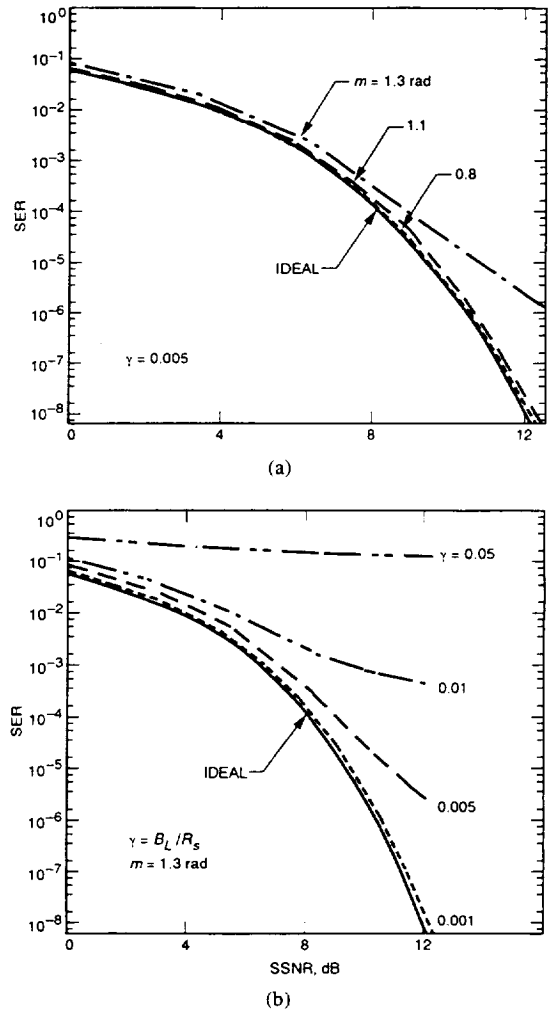

Fig. 9. SER for PCM/PM/NRZ. (a) SER versus SSNR for PCM/PM/NRZ ($\gamma = 0.005$). (b) SER versus SSNR for PCM/PM/NRZ ($m = 1.3$ rad).

i.e., by either increasing the data rate or by decreasing the loop noise bandwidth. For Fig. 9(a) and (b) to be useful, they must be used in the operating region of the PLL, as given earlier in Fig. 5(a) and (b). For example, when $\gamma = 0.01$ and $m = 1.3$ rad, Fig. 5(b) indicates that the PLL locks, provided that the SSNR is at least 8 dB. Therefore, when using the performance curve corresponding to the above operating conditions, such as Fig. 9(b), only the region where the SSNR $\geq$ 8 dB is useful.

b) Very Low-Data-Rate Case: When the data rate is low relative to the receiver tracking loop bandwidth, the phase process $\phi(t)$ varies rapidly over the symbol interval T_S. Hence, the random variable $Y(\phi)$, as given in (41), is a good approximation of the true time average of the function $\cos\left[\phi(t)\right]$. When $\phi(t)$ can be modeled as an ergodic process, the time average may be replaced by the statistical mean. Thus

$$Y(\phi) \simeq E\{\cos\phi\} = \int_{-\pi}^{\pi} \cos\phi p(\phi) d\phi = C_0. \tag{45}$$

The constant C_0 can be computed by substituting the expression for the pdf of the phase error derived from (37) in (45). Then, by substituting in (41) and (43) one obtains the average

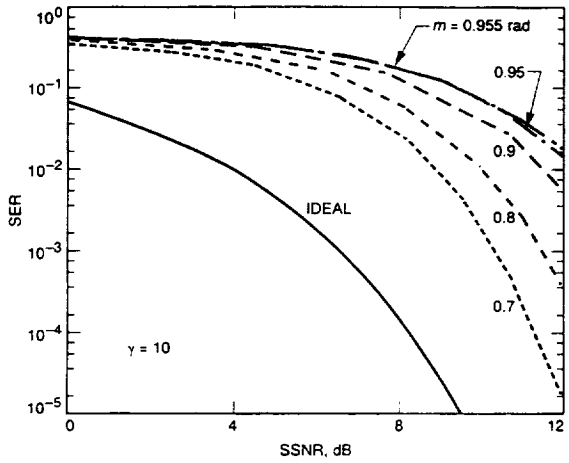

Fig. 10. SER versus SSNR for PCM/PM/NRZ ($\gamma = 10$), low-data-rate case.

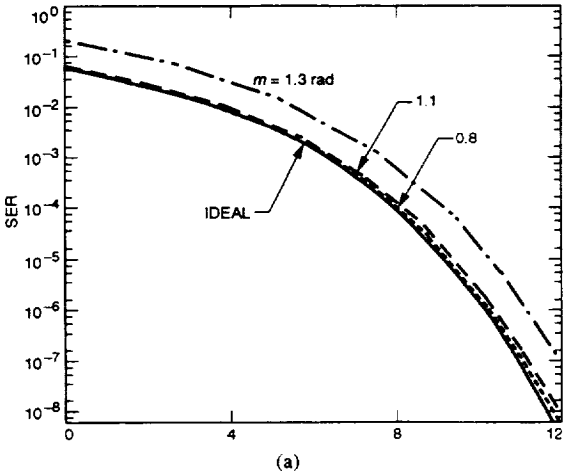

(a)

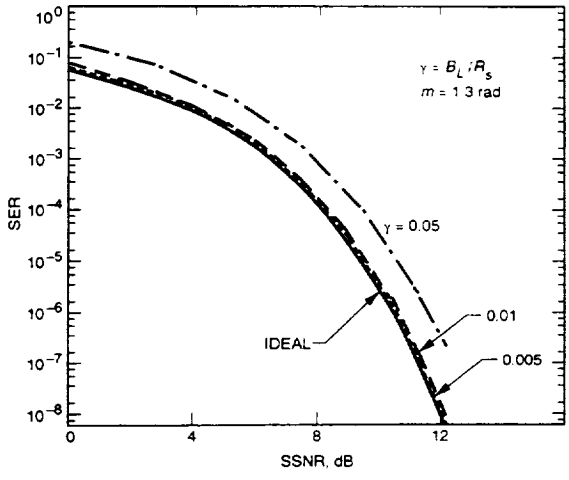

(b)

Fig. 11. SER versus PCM/PM/bi-phase. (a) SER versus SSNR for PCM/PM/bi-phase ($\gamma = 0.05$). (b) SER versus SSNR for PCM/PM/bi-phase ($m = 1.3$ rad).

symbol error probability

$$P_S = \frac{1}{2}\,\mathrm{erfc}\left(\sqrt{\frac{E_S}{N_0}}C_0.\right) \tag{46}$$

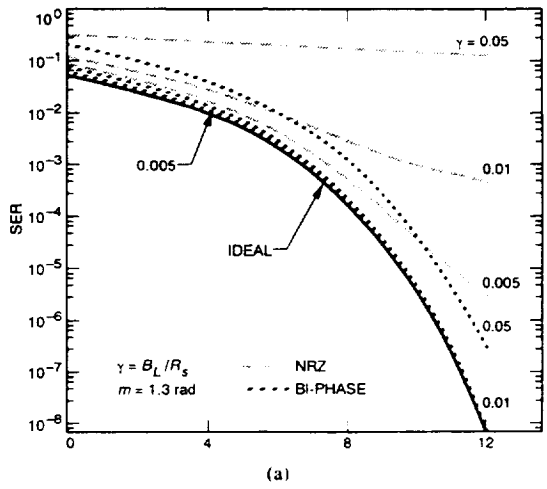

(a)

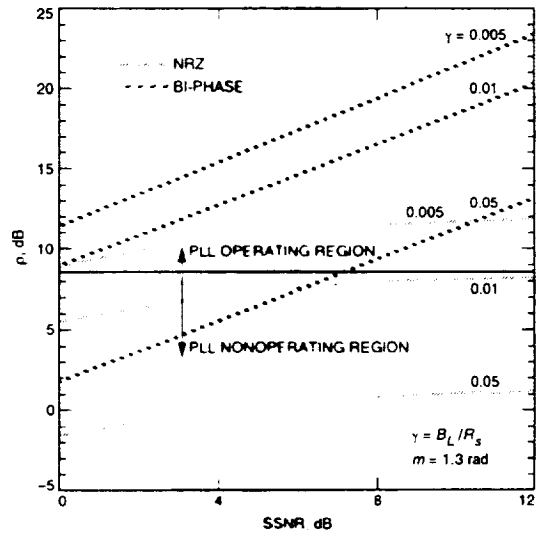

(b)

Fig. 12. Performance composition of PCM/PM/NRZ and PCM/PM/bi-phase. (a) SER versus SSNR for PCM/PM when $m = 1.3$ rad. (b) Effective loop SNR versus SSNR for PCM/PM when $m = 1.3$ rad.

In Fig. 10, P_S is plotted as a function of SSNR for different values of m when $\gamma = 10$. The figure shows that the degradation is substantial and becomes worse as m increases. It should be noted that the approximation used is valid when ICR < 1, which corresponds to $m \leq 0.9551$ rad. However, Fig. 6 indicates that in order for the PLL to maintain lock, one must operate at an SSNR higher than 20 dB, even for the smallest modulation index chosen (0.7 rad), an impractical requirement to say the least. Therefore, the PCM/PM modulation technique with the NRZ data format is not a viable choice when $B_L \geq R_S$.

2) PCM/PM with Bi-phase Data Format: Assuming that the data rate is high, i.e., $\gamma < 0.1$, the random variable $Y(\phi)$ is approximated as in (43). By substituting the result and the appropriate Tikhonov pdf for this case, as derived in (42), one obtains an expression for the SER. This average SER is calculated as a function of the SSNR E_S/N_0 for different values of m when $\gamma = 0.05$, and the results are plotted in Fig. 11(a). One observes that a noticeable degradation occurs

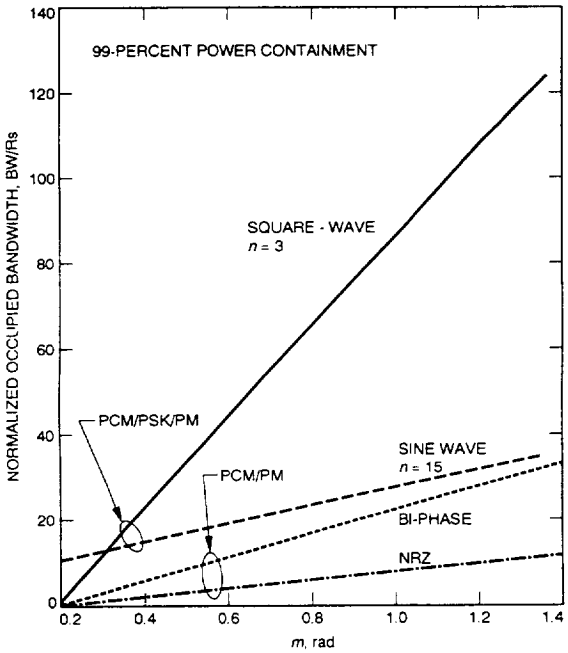

Fig. 13. Bandwidth occupancy of PCM/PSK/PM versus PCM/PM signals.

TABLE I
CRITICAL VALUES OF γ_{CR}

Modulation Index (rad)	γ		
	PCM/PM/NRZ	PCM/PM/Bi-phase	PCM/PSK//PM $n = 3$
0.9	0.019	0.268	any value
1.3	0.002	0.09	0.56

TABLE II
SSNR DEGRADATION WHEN $\gamma = 0.001$ AND $m = 1.3$ rad

SER	SSNR Degradation (dB)		
	PCM/PM/NRZ	PCM/PM/Bi-phase	PCM/PSK/PM $n = 3$
10^{-3}	0.04	negligible	negligible
10^{-4}	0.06	negligible	negligible
10^{-5}	0.09	negligible	negligible

TABLE III
SSNR DEGRADATION WHEN $\gamma = 0.005$ AND $m = 1.3$ rad

SER	SSNR Degradation (dB)		
	PCM/PM/NRZ NRR*	PCM/PM/Bi-phase	PCM/PSK/PM $n = 3$
10^{-3}	0.5	negligible	negligible
10^{-4}	0.7	negligible	negligible
10^{-5}	1.2	negligible	negligible

*NRR in the column corresponding to the PCM/FM/NRZ scheme refers to not recommended region, because the chosen value for γ is greater than the critical value for this scheme (see Table I). Therefore, serious degradation for that particular scheme is observed.

TABLE IV
SSNR DEGRADATION WHEN $\gamma = 0.005$ AND $m = 1.1$ rad

SER	SSNR Degradation (dB)		
	PCM/PM/NRZ NRR*	PCM/PM/Bi-phase	PCM/PSK/PM $n = 3$
10^{-3}	0.10	negligible	negligible
10^{-4}	0.15	negligible	negligible
10^{-5}	0.20	negligible	negligible

*NRR = not recommended region.

only for the case when $m = 1.3$ rad. The effect of varying γ is shown in Fig. 11(b) for $m = 1.3$ rad. When $\gamma = 0.005$, the performance of the loop SNR approaches that of the ideal case.

3) PCM/PSK/PM: By substituting the calculated phase error variance obtained in Section III-B.3 and (42), it is found that when the integer $n \geq 3$, the performance approaches that of the ideal case. Whereas when $n = 1$, the performance is identical to the PCM/PM scheme with the bi-phase data format case, as it should be.

IV. DISCUSSION AND SUMMARY OF THE RESULTS

A. Theoretical Results

The critical values of γ for a given modulation index for which the ICR exceeds the CCIR recommended threshold value of -15 dB are obtained. These values are given in Table I for all the schemes when $m = 0.9$ and 1.3 rad.

From Table I, one notes that for a given modulation index, the PCM/PM scheme with the NRZ data format requires a value of γ smaller than the other two schemes to operate at the threshold interference level. The PCM/PSK/PM scheme performs just as well at a much larger γ ratio when $n = 3$ or higher.

The SER and the effective loop SNR of the PCM/PM scheme with both NRZ and bi-phase data formats, as well as the ideal case, are superimposed in Fig. 12(a) and (b) when $m = 1.3$ rad for different values of γ, in order to compare their performance. The criterion is the degradation in SSNR for the particular scheme considered relative to the ideal case, i.e., the required increase in SSNR in order to achieve the same performance as the ideal case. This degradation is due to both the thermal noise and the data interference. The SSNR degradation of the three schemes considered is obtained for different values of m and γ from the figures and is summarized in Tables II–V.

In Table II, the chosen value for γ is very small and is below the critical value (see Table I) for all the schemes. One notes a very small degradation for the PCM/PM/NRZ scheme and negligible degradation for the other two schemes. Table III shows the effects of increasing γ.

In Table IV, the dependence of the performance on the modulation index is demonstrated. The loop bandwidth-to-data rate ratio is unchanged from the previous table, but the modulation index is smaller. It is observed that the performance of the PCM/PM/NRZ scheme improves as the modulation index decreases.

In Table V, both PCM/PM schemes are in the not-recommended region (NRR) (see Table I). The two PCM/PM schemes can be compared in terms of the effective loop SNR for the same values of SSNR, m and γ. The scheme with the

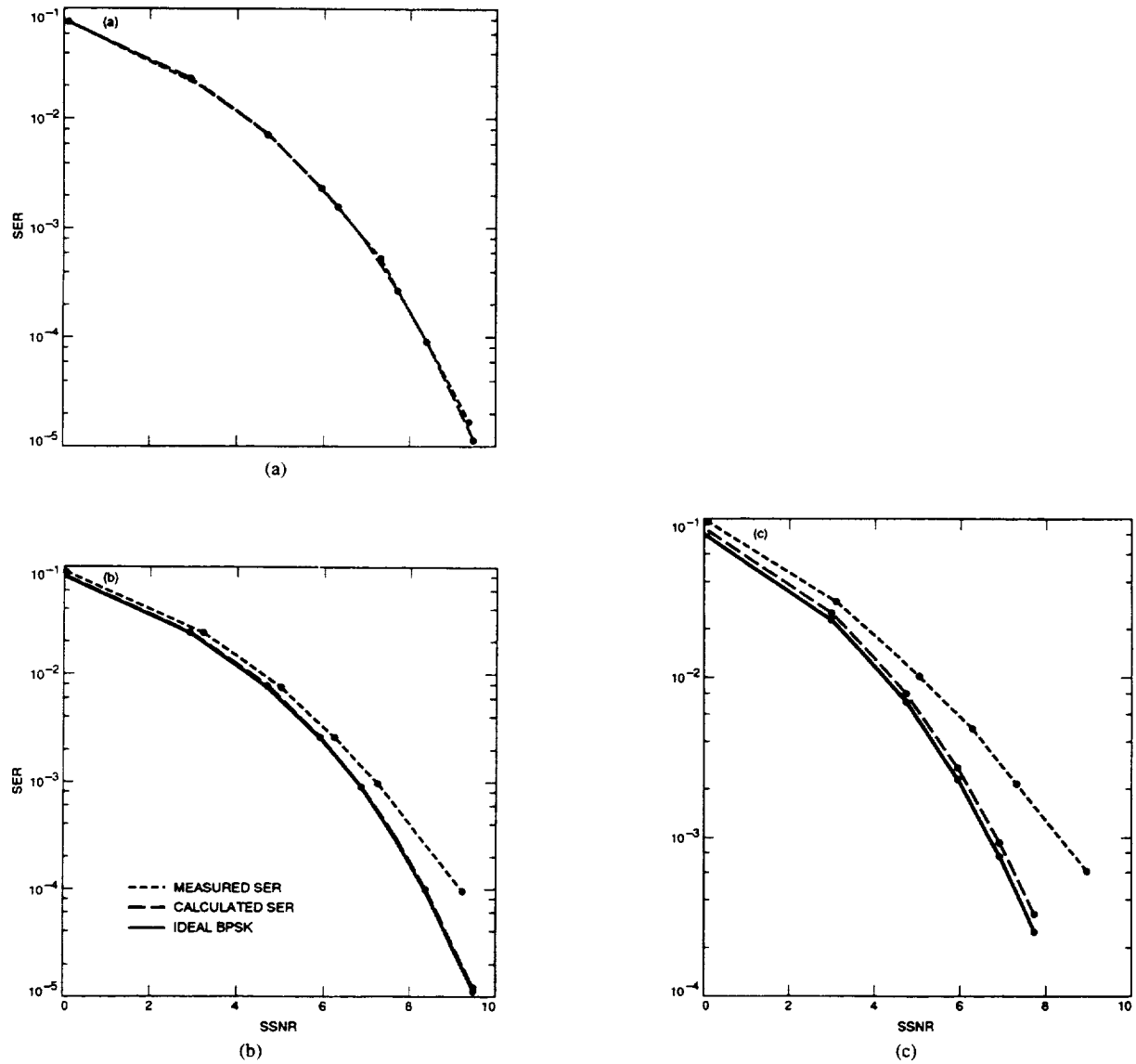

Fig. 14. Measured performance for PCM/PM/NRZ. (a) ICR = −24 dB (m = 1.1 rad, γ = 0.001). (b) ICR = −18.6 dB (m = 1.3 rad, γ = 0.001). (c) ICR = −15.8 dB (m = 1.3 rad, γ = 0.002).

TABLE V
SSNR DEGRADATION WHEN γ = 0.05 AND m = 1.3 rad

SER	SSNR Degradation (dB)		
	PCM/PM/NRZ	PCM/PM/Bi-phase	PCM/PSK/PM $n = 3$
10^{-3}	NRR* PLLNOR**	1.2 (NRR)	NEGLIGIBLE
10^{-4}	NRR PLLNOR	1.1 (NRR)	NEGLIGIBLE
10^{-5}	NRR PLLNOR	1.05 (NRR_	NEGLIGIBLE

*NRR = not recommended region.
**PLLNOR = PLL nonoperating region (ρ < 8 dB).

TABLE VI
EFFECTIVE LOOP SNR WHEN m = 1.3 rad AND SSNR = 7 dB

γ	Effective Loop SNR, ρ (dB)	
	PCM/PM/NRZ	PCM/PM/biphase
0.050	1.0 (NRR*, PLLNOR**)	9.0 (NRR)
0.010	8.0 (NRR)	16.0
0.005	11.5 (NRR)	19.0
0.001	18.0	25.9

*NRR = not recommended region.
**PLLNOR = PLL nonoperating region (ρ < 8 dB)

higher effective loop SNR performs better. Using Figs. 5(b) and 7(b), the values are tabulated in Table VI. It is observed that for the same operating parameters, the PCM/PM/bi-phase scheme always has a higher effective loop SNR than the PCM/PM/NRZ scheme.

The unfiltered occupied bandwidth with 99% power containment as a function of the modulation index for both PCM/PSK/PM and PCM/PM signals is derived in [9]. The results are summarized here in Fig. 13. As expected, it is shown that the PCM/PM scheme with the NRZ data format requires the least occupied bandwidth and the PCM/PSK/PM scheme requires the most. The bandwidth occupancy increases linearly with the modulation index for all the schemes.

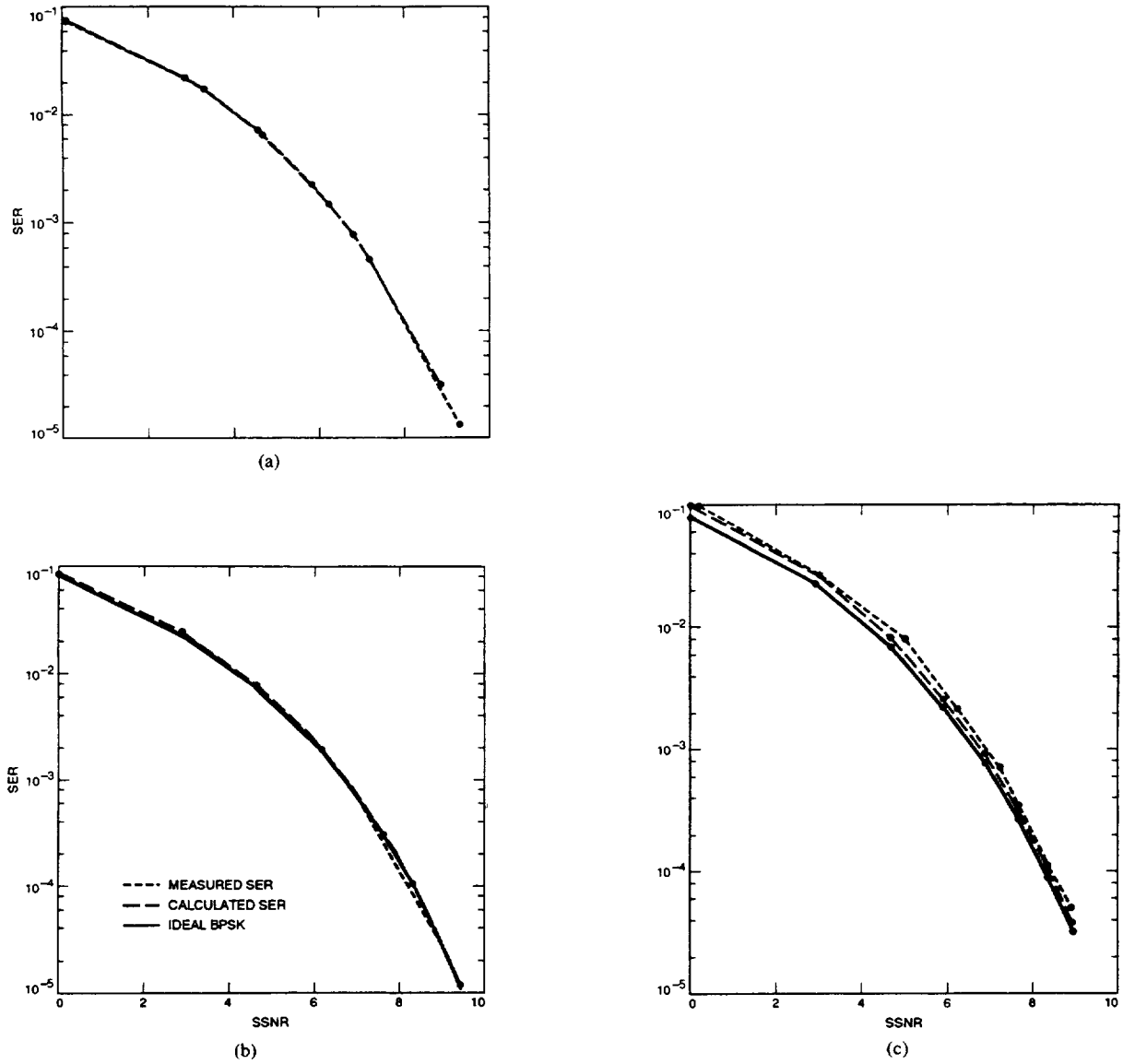

Fig. 15. Measured performance for PCM/PM/bi-phase. (a) ICR = −59.5 dB (m = 1.1 rad, γ = 0.001). (b) ICR = −54.2 dB (m = 1.3 rad, γ = 0.001). (c) ICR = −40.2dB (m = 1.3 rad, γ = 0.005).

B. Measured Performance

The measured SER values for all schemes were obtained by using the Advanced Receiver (ARX) II. A functional description of the ARX II is presented in [10]. Fig. 14(a)–(c) depicts the measured performance for the PCM/PM/NRZ signal when the ICR = − 24 dB, − 18.6 dB, and − 15.8 dB. It is clear that the model predicts the measurements for ICR < − 15 dB. As the ICR increases, the measurements diverge from the model, as shown in Fig. 14(c). The same observations are reported for the PCM/PM/bi-phase signal type, as evident in Fig. 15(a)–(c). However, for this signal type the deviation of the measured values from the theoretical values is less than that of the NRZ signal type for the same m and γ. The above deviations indicate that the assumptions made to regard the data interference as additional white noise are valid as long as γ is less than a threshold value, as specified in Table I. Fig. 16 indicates that for the PCM/PSK/M case, the measured performance is identical to the theoretical performance when m = 1.1 rad and γ = 0.001.

V. Conclusion

In this paper, the performance of the PCM/PM/NRZ scheme has been considered in the limiting two cases of high- and very-low-data rates and the performance of PCM/PM/bi-phase scheme was considered for the high-data-rate case and compared with the PCM/PSK/PM scheme. As long as the PLL implementation by the DSN is used, the following conclusions are valid. In terms of SER performance, the PCM/PSK/PM scheme is better than the PCM/PM scheme (both NRZ and bi-phase) when the loop bandwidth-to-data rate ratio is not small enough, as discussed in the previous section. However, the PCM/PSK/PM scheme requires a great deal of bandwidth. In terms of bandwidth efficiency, the PCM/PM/NRZ scheme is the best but has higher degradation for $\gamma \geq 0.001$ and m = 1.3

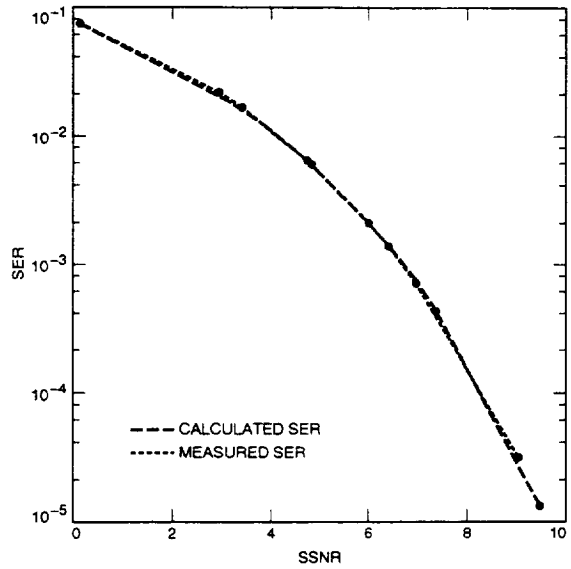

Fig. 16. Measured SER for PCM/PSK/PM with square-wave subcarrier $m = 1.1$ rad and $\gamma = 0.001$.

rad. As a compromise, the PCM/PM/bi-phase scheme can be used with twice the bandwidth of the PCM/PM/NRZ scheme but with much less degradation. However, at a very small loop bandwidth-to-data rate ratio, which at present the DSN receivers are capable of supporting, the performance of the PCM/PM schemes coincides with that of the PCM/PSK/PM scheme. In addition, if one takes into account the subcarrier loss in the receiver when the PCM/PSK/PM scheme is employed, the performance of PCM/PM schemes becomes as good as, if not better than, that of the PCM/PSK/PM scheme. Moreover, under these conditions the PCM/PM/NRZ scheme becomes the most attractive because it requires the least bandwidth occupancy. If PLL-based receiver implementation is not required, then the BPSK scheme without a residual carrier is most attractive.

ACKNOWLEDGMENT

The authors wish to thank Dr. V. Vilnrotter and anonymous reviewers for all of their valuable comments and B. Goforth for her help in preparing this paper for submission.

REFERENCES

[1] J. Yuen, Ed., *Deep Space Telecommunications Systems Engineering*. New York: Plenum, 1983.
[2] Consultative Committee for Space Data Systems, *Recommendations for Space Data System Standards, Radio Frequency and Modulation Systems, Part I, Earth Stations and Spacecraft*, CCSDS 401.0-B, Blue Book, Washington, DC: NASA, CCSDS Secretariat, Communications and Data Systems Division (Code OS), 1989.
[3] J. K. Holmes, *Coherent Spread Spectrum Systems*. New York: Wiley, 1982.
[4] T. M. Nguyen, "Closed form expressions for computing the occupied bandwidth of pcm/psk/pm signals," in *Proc. IEEE Int. Symp. on EMC* (Cherry Hills, NJ, Aug. 1991).
[5] International Radio Consultative Committee (CCIR), "Protection criteria and sharing considerations relating to deep space research," Rep. 685–2, in *Recommendations and Reports of the CCIR, XVIth Plenary Assembly, Volume II: Space Research and Radio Astronomy* (Dubrovnik, Yugoslavia), 1986, pp. 278–289.
[6] W. C. Lindsey and M. K. Simon, *Telecommunications Systems Engineering*. Englewood Cliffs, NJ: Prentice-Hall, 1973.
[7] T. M. Nguyen, "Space telemetry degradation due to manchester data asymmetry induced carrier tracking phase error," *IEEE Tran. Electromagn. Compat.*, vol. 33, no. 3, pp. 262–268, Aug. 1991.
[8] C. Y. Youn and W. C. Lindsey, "Phase-locked loop performance in the presence of CW interference and additive noise," *IEEE Trans. Commun.*, vol. COM-30, no. 10, pp. 2305–2311, Oct. 1982.
[9] T. M. Nguyen, "Occupied bandwidths for PCM/PSK/PM and PCM/PM signals—A comparative study," in *CCSDS Subpanel 1E*, RF and Modulation Meeting, Salzburg, Austria, May 1992.
[10] S. M. Hinedi, "NASA's next generation deep space network breadboard receiver," *IEEE Trans. Commun.*, vol. 41, no. 1, pp. 246–257, Jan. 1993.

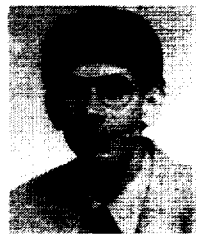

Mazen M. Shihabi (S'87) was born in Aleppo, Syria. He received the B.S.E.E., M.S.E.E., and E.E.E. degrees, all from the University of Southern California, Los Angeles, in 1984, 1986, and 1987, respectively. He is currently pursuing the Ph.D. degree at the University of California, Irvine.

From 1988 to 1990, he was with Master Electronic Controls, Santa Monica, CA, where his work involved hardware design and implementation of digital timing devices. Since June 1990, he has been with the Communications Systems Research Section of the Jet Propulsion Laboratory, Caligornia Institute of Technology, Pasadena. His current research interests include digital communications systems, parameter estimation in dynamic environments, as well as time–frequency and time–scale transforms.

Mr. Shihabi is a member of Eta Kappa Nu.

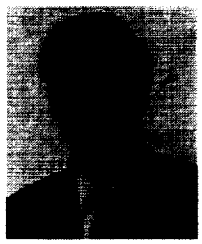

Tien Manh Nguyen (S'78–M'83–SM'93) received the A.A., B.S.E., and M.S.E. degrees (specializing in electromagnetic field theory) from Fullerton College and California State University, Fullerton (CSUF), in 1978, 1979, and 1980, respectively. A doctoral candidate at the University of California, San Diego (UCSD) from 1980 to 1983, he completed all course requirements for the Ph.D. degree and received the M.S.E.E. degree (specializing in communication theory and systems) in 1982. He received the Ph.D. degree in electrical engineering from Columbia Pacific University, San Rafael, CA, in 1986. He also received the M.A. degree in mathematics from the Claremont Graduate School, Claremont, CA, in 1993.Currently he is pursuing the Ph.D. degree in engineering mathematics at the Claremont Graduate School jointly with California State University at Long Beach (CSULB).

He has been a Certified Manufacturing Technologist since 1984 and certified EMC Engineer since 1990. He was also a Student Assistant at CSUF from 1978 to 1980, and a Teaching Assistant at UCSD between 1982 and 1983. In 1983 he joined ITT Educational Services Inc., where he became chief of the Automated Manufacturing Department. While at ITT he also taught modern electronic communications and microwave courses. From 1985 to 1990, he was with the Communications Systems Section and since January 1991, he has been a member of the Technical Staff of the Communications Systems Research Section, Jet Propulsion Laboratory, Pasadena, CA. His current interests include integral transforms, statistical decisions, digital communications systems, parameter estimation, and digital signal processing. He was a Vice-Chairman of IEEE/EMC/TC6 and was Session Chairman of the 1986 IEEE/EMC International Symposium. Since 1986 he has served as a NASA/JPL delegate to the Consultative Committee for Space Data Systems (CCSDS). He was a recipient of a San Diego Fellowship Award for 1980–1982 and also received an IEEE/EMC Award in 1986, the Bendix Management Club Award in 1987, a Certificate of Accomplishment from the Manufacturing Engineering Certification Institute in 1988, a NASA Group Achievement Honor Award in 1988, more than a dozen of NASA certificates of recognition, and holds one patent. He is a recipient of the CSULB Foundation Award for 1991–1992. He served as the Editor for the CCSDS *Green Book, RF and Modulation*, 1989, and *Yellow Book* 1994.

Dr. Nguyen is a member of the New York Academy of Sciences, AMS, Phi Kappa Phi, and a senior member of AIAA.

Sami Hinedi (M'83) was born in Aleppo, Syria, on May 27, 1963. He received the B.S.E.E., M.S.E.E, and Ph.D. degrees, all from the University of Southern California, Los Angeles, in 1983, 1984, and 1987, respectively.

Since June 1987, he has been in the Communications Systems Research Section of the Jet propulsion Laboratory, Pasadena, CA, where he is currently the supervisor of the Digital Signal Processing Research Group. His current interests include spread spectrum communications, parameter estimation in dynamic environments, modem receiver design, and digital signal processing.

Dr. Hinedi is a member of Eta Kappa Nu.